Ultraviolet-photoemission and electron-energy-loss spectroscopic studies of ^{99}Tc

T.-P. Chen and E. L. Wolf
Ames Laboratory—U.S. Department of Energy, Iowa State University, Ames, Iowa 50011

A. L. Giorgi
Los Alamos National Laboratory, Los Alamos, New Mexico 87545
(Received 25 July 1983; revised manuscript received 23 January 1984)

Angle-integrated ultraviolet-photoemission and reflection electron-energy-loss spectra have been obtained for ^{99}Tc for the first time. The photoemission energy distribution curves are in semiquantitative agreement with the calculated density of states. The work function of this material was found to be 5.0±0.5 eV. The volume and surface plasmons are at 25.0±0.5 and 20.7±0.5 eV, respectively. A lower plasma oscillation is observed at 9.5±0.5 eV. $N_{\rm I}$ and $N_{\rm II,III}$ ionization energies obtained are in good agreement with x-ray measurements. Comparisons of ^{99}Tc properties to those of other transition metals in period 5 are also given.

I. INTRODUCTION

Technetium (Tc) is an interesting element in that, although its atomic number is only 43, it has no stable isotopes and is the unique radioactive element among the transition metals. For this reason relatively few data are available for this element. However, Tc is the center element in the second group of transition metals. Therefore, the lack of experimental data on this element may lead to difficulties in visualizing the trend of physical properties for the group.[1] Tc is also a high-temperature superconducting element with a transition temperature close to 8 K.[2] This is next only to niobium [$T_c=9.2$ K (Ref. 3)] and is the highest T_c among all elements of hcp crystal structure. Superconductivity is generally believed to arise from the electron-phonon interaction. The coupling parameter λ of the interaction depends on the electronic structure near the Fermi energy in a complex and incompletely understood fashion. A study in the electronic structure of superconducting materials may yield not only information about the electronic properties of the material but also a better understanding of their superconducting properties. In fact, Papaconstantopoulos *et al.*[4] have used their band-structure results to calculate λ and T_c for 32 metals including technetium. Unfortunately, a bcc crystal structure was assumed for technetium in their calculation, which results in a very low transition temperature, viz. 0.03 K, in contradiction to the experimental result. The band structure of Tc using three different crystal potentials and the hcp lattice was reported recently by Asokamani *et al.*[5] A density-of-states histogram, using the Vashista and Singwi exchange and correlation scheme, was also provided.

The ultraviolet-photoemission spectrum (UPS) and the electron energy loss spectrum (EELS) are sources of information on the electronic structure of materials. In UPS one measures the energy distribution curve (EDC) of the photoelectrons emitted from the sample irradiated with photons of energy $\hbar\omega$. The detected number of photoelectrons of kinetic energy E_k is proportional to the joint density of states (JDOS) of escaped electrons of initial energy $E_F-(\hbar\omega-\phi_s-E_k)$, where ϕ_s is the sample work function. The structure in the EDC would therefore correlate with the initial density of states of the electron in the sample. Lindau and Spicer[6] have demonstrated that the work function ϕ_s can also be obtained from the high- and low-energy cutoffs of the EDC in photoemission measurements.

The EELS provides information on the collective electronic motion—the plasma oscillations as well as the interband transitions and core-level ionization energies. In a free electron model the volume plasmon occurs at the energy[7]

$$\hbar\omega_p=\hbar\left[\frac{4\pi Ne^2}{m}\right]^{1/2}, \tag{1}$$

and the surface plasmon at the energy[8]

$$\hbar\omega_{sp}=\frac{\hbar\omega_p}{\sqrt{2}} \tag{2}$$

for a thick sample. Here N is the electron density, e the electron charge, m the electron mass. Experimental results generally show good agreement with what is predicted by Eq. (1), but not by Eq. (2).[9]

Weaver, Lynch, and Olson[10–13] have reported careful measurements of both volume and surface energy-loss functions[14] on a variety of transition metals. Figure 1 shows the surface and volume loss functions for Nb determined by Weaver, Lynch, and Olson.[10] In their measurements, the features of the loss functions for the period-5 transition metals, Zr, Nb, Mo, and Rh, are similar. They all have two pronounced peaks in both the volume and surface loss functions as indicated in Fig. 1. The high-energy peaks can be associated with the volume and surface plasmons as predicted by Eqs. (1) and (2). The lower energy peaks, on the other hand, do not follow these equations unless the value of electronic density N is reduced. This led them to argue that the volume plasmon at lower energy probably involves only a group of electrons;

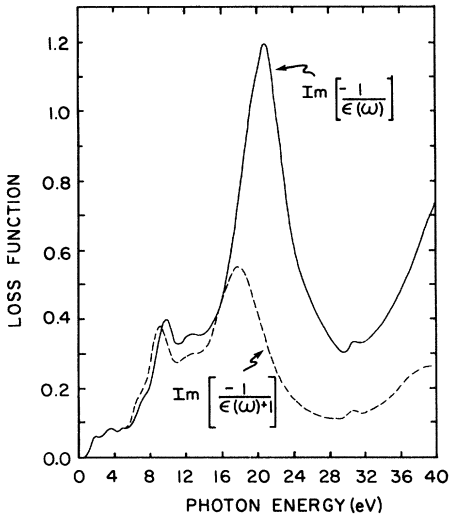

FIG. 1. Volume and surface energy-loss functions of niobium as determined by Weaver, Lynch, and Olson (Ref. 10) from ultraviolet optical studies. The volume loss function $\mathrm{Im}(-1/\epsilon)$ is shown as a solid line, the surface loss function $\mathrm{Im}[-1/(\epsilon+1)]$, dashed.

perhaps the core charge density of the *d*-like electrons does not participate. Schubert and Wolf[15] measured electron energy loss spectra of vanadium, niobium, molybdenum, and tantalum and demonstrated empirically a direct mapping of spectral features in the low-energy region of reflection EELS into peaks in the volume and surface energy loss functions determined by Weaver *et al.* in their optical studies.[10–13]

In addition to these points, plasma oscillations are interesting for the following reasons: First, the question of screening the electron-phonon interaction by collective electron motion is regarded[16] as a central difficulty, in the accurate calculation of the electron-phonon coupling constant λ, of importance in superconductivity. Second, there is the recent restatement[17] of Fröhlich's suggestion[18] that screening of *d*-electron plasma oscillations by *s* electrons may allow the formation of an acoustic plasmon branch which could supplement or replace the electron-phonon interaction leading to superconductivity. Third, the collective properties, in contrast to one-electron properties, seem to present greater difficulty in theoretical calculation. For example, the plasma energies[19,20] calculated theoretically for niobium are not in good agreement with EELS or UV optical studies.

II. EXPERIMENTAL METHOD

The experimental setup and method of sample preparation in our EELS measurement of ^{99}Tc are the same as that of our Auger electron studies and have been published elsewhere.[1] However, for completeness, we will briefly discuss the experimental procedure here. A $0.002\times0.50\times1.0$ in. ^{99}Tc foil was mounted on a Varian precision sample manipulator in an ultrahigh-vacuum (UHV) chamber with a base pressure $\lesssim1\times10^{-10}$ Torr. The basic features of our UHV system are similar to those described by Shen.[21] The metal foil was heated repeatedly to approximately 2000 °C until clean, as determined from Auger spectroscopy.[1] The reflection EELS was taken with a double-pass cylindrical mirror analyzer (CMA) used in a preretarded mode to obtain sufficient energy resolution (±0.3 eV). Each run consisted of three EELS traces, an EDC and its first and second derivatives, measured immediately after Auger analysis to monitor the surface cleanliness. Most of our data were taken with the electron energy set at 500 eV, although other settings (200, 300, 400, and 1000 eV) have been used. Since no significant change in the EDC was found, we shall thus report only the data taken with a primary energy of 500 eV.

In ultraviolet-photoemissin-spectroscopy (UPS) measurements, a differentially pumped, windowless, microwave excited, noble gas discharge lamp[22] was used. The first ionization lines of helium gas (He I with energy $\hbar\omega=21.2$ eV) and neon gas (Ne I with energy $\hbar\omega=16.8$ eV) were used to excite electrons in the sample. The sample and electron collection geometry is sketched at the upper left in Fig. 2. The collection cone of the CMA opens at an angle 42.3° about the positive *y* axis. The UPS light (wavy line) is incident at approximately 38° to the foil normal, at an angle of 83° to the CMA axis, and at an angle 20° to the *y*-*z* plane. Electrons from a PHI Model 04-015 grazing incidence electron gun are incident on the sample from a direction symmetrically located with respect to the *y*-*z* plane, at an angle 20° from its opposite side.

The UPS energy resolution is 0.35 eV for all EDC's excepting the dashed curve of Fig. 3, at 1.4-eV resolution,

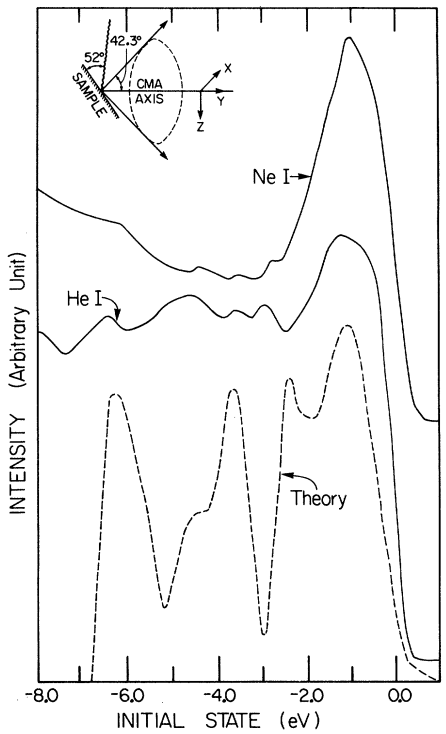

FIG. 2. Photoemission EDC's from E_F to 8 eV below for ^{99}Tc taken at excitation energies 21.2 eV (He I) and 16.8 eV (Ne I) are shown as solid lines. Density of states calculated by Asokamani *et al.* (Ref. 5) is shown in dashed line for comparison.

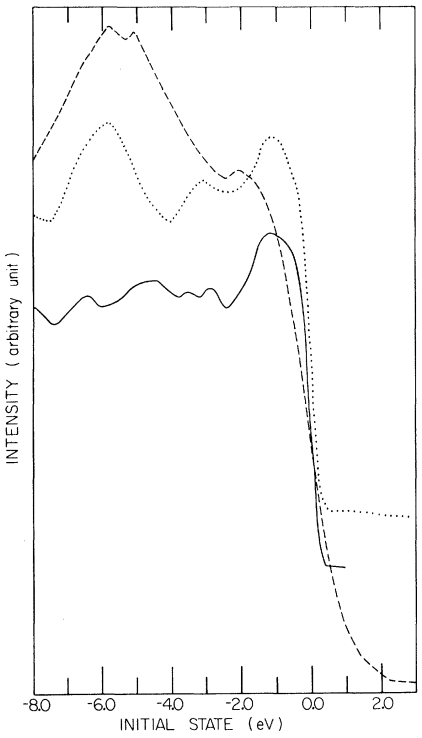

FIG. 3. Photoemission EDC's for clean (solid line) ^{99}Tc, for ^{99}Tc contaminated by residual gases (dotted line), and for ^{99}Tc contaminated by pure oxygen (dashed line).

and the Ne I curve in Fig. 4 taken at 0.2-eV resolution. Before data taking, the base pressure of the chamber was $\leq 1\times10^{-10}$ Torr. During data taking, the equilibrium pressure of the chamber was $\leq 2\times10^{-9}$ Torr for He I excitation with the gas pressure of the lamp set at 0.2 mTorr and $\leq 6\times10^{-10}$ Torr for Ne I excitation with gas pressure set at 0.1 mTorr. The balance was achieved by pumping out the noble gas, which had flowed into the chamber from the discharge lamp. For comparison purposes, EDC's have also been taken on samples contaminated in two different ways. For the first, we left a clean sample

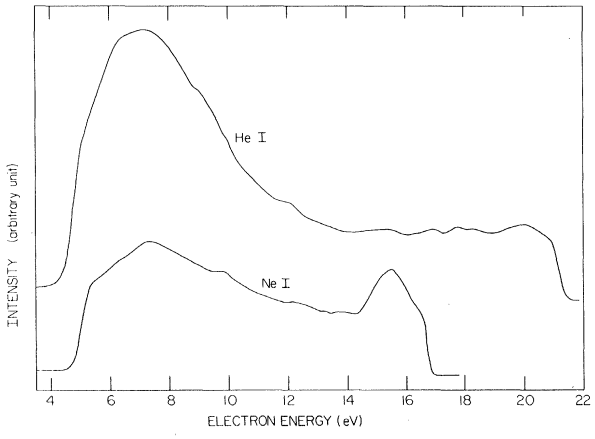

FIG. 4. Full photoemission EDC's for ^{99}Tc obtained using the first excitation lines of He and Ne. The work functions obtained from these curves are 4.9±0.4 eV and 5.1±0.2 eV for He I and Ne I, respectively. The sample was biased by −5.0 V with respect to the collector of the CMA.

in the UHV chamber with a background helium pressure (from the discharge lamp) of $\sim 2\times10^{-9}$ Torr for 5 h before EDC traces were taken. In the second, pure oxygen gas was admitted into the chamber and the clean foil was exposed to 180 L (1 L = 1 langmuir = 10^{-6} Torr sec) of pure oxygen at room temperature. A Varian UHV-24 ionization gauge and a UTI model AGA-100 MUX gas analyzer head installed in the chamber were the only possible sources for ionization of the admitted molecular oxygen. The gas analyzer indicated about 10% atomic oxygen.

III. RESULTS AND DISCUSSION

A. UPS

In Fig. 2 we display our angle-integrated EDC's (solid lines) of ^{99}Tc using He I and Ne I photons for excitation. The gain in the He I excited curve had been increased by a factor of 3 over that of the Ne I measurements resulting in a larger signal in the EDC. Five peaks were observed in the energy region between the Fermi level and 8 eV below. The energy widths of the EDC's are determined using the mean energies between the 10% and 90% points on the sharp rise and sharp drop of the EDC. The most intense peak occurs at 1.1 eV and subsequent peaks lie at 2.7, 3.5, 4.5, and 6.3 eV below the Fermi energy. The density of states (DOS) calculated by Asokamani *et al.*[5] is also shown in Fig. 2 (by dashed line) for comparison. The overall agreement between the calculated DOS and measured EDC are good, except for the peak at −2.7 eV which appears to be ~ -2.3 eV (Ref. 23) in the calculated DOS. In addition, the shoulder at around −4.5 eV in the DOS appears to be a peak in the EDC.

The solid line in Fig. 3 is the EDC of clean ^{99}Tc, the dashed line is that of the sample oxidized by pure oxygen, while the dotted curve is the trace from a contaminated sample after it has been left inside the chamber for 5 h without Joule heating. These curves exhibit significant differences. Almost all of the structure in the EDC of the clean sample is washed out after it is contaminated, except for the most pronounced peak at 1.1 eV, which is seen to be shifted to a lower energy. At the present time, we are not clear about the origin of the weaker peak at −3.0 eV (on the dotted curve). However, the quadrupole mass analyzer indicated 60% of the residual gas at 1×10^{-10} Torr base pressure was hydrogen related, namely H, H_2, and H_2O. The sample, therefore, was exposed to 1 L of hydrogen after 5 h in the vacuum chamber. Experiments on hydrogen adsorbed by transition metals have reported that the adsorption of H atoms on the metal will introduce H-induced states.[24–32] The induced states appear at a coverage as low as a few tenths of 1 L. Smith[28] further reported that for Nb the induced peak grew to 40% of its saturation amplitude at 1 L. The energy level of the induced states are different for different materials. For Nb the induced level was found to be −1.8 eV,[28] for Mo they are −2.0, −4.0, −5.3, and −7.0 eV,[29] while for Pd it is reported to be around −6.5 eV by Conrad[30] and Demuth[25] and −5.4 eV by Eastman *et al.*[27] The −3.0-eV peak of Tc is therefore possibly a H-induced level similar to those of the other 4*d* metals Nb, Mo, and Pd.

The peak at 6.0 eV below E_F comes mostly from the oxygen $2p$ level, and is commonly found on metals with low oxygen surface coverage. This peak grows and splits into two when the amount of oxygen on the sample is increased, as is indicated in the dashed curve. The broadening and splitting of the peak has been attributed to the formation of surface oxide with a corresponding oxygen $2p$ derived valence band structure.[33]

Figure 4 shows full energy distribution curves for both Ne I and He I excitation. A -5.0-V bias was applied to the sample during the course of tracing these curves. The energy ranges of these EDC's are estimated to be 11.7 ± 0.2 eV for Ne I and 16.3 ± 0.4 eV for He I. These are obtained by subtracting the low-energy cutoff $(\phi_s-\phi_c)$ from the high-energy cutoff $(\hbar\omega-\phi_c)$ on the EDC. Here ϕ_s and ϕ_c are the sample and collector work functions, respectively. The work functions ϕ_s calculated by using $\hbar\omega-\phi_s=$energy range of EDC and the above data are 5.1 ± 0.2 eV for Ne I excitation and 4.9 ± 0.4 eV for He I excitation (as a check we have applied the same technique and analysis to a pure Au sample and found a ϕ_s value of 5.2 ± 0.3 eV in agreement with literature values). The average ϕ_s value for ^{99}Tc is 5.0 ± 0.5 eV. To our knowledge there is no work-function measurement of technetium prior to this experiment. Trasatti[34] made a semiempirical calculation and obtained a value of 4.9 eV. Michaelson[35] estimated a value of 4.4 eV for this element from the trend of measured work-function values for neighboring transition metals of Tc. However, improvements in both instrumentation and experimental technique show that a number of work-function values cited in Michaelson's paper now appear to be not very reliable. More recent data show work-function values for Nb ranging from 4.19 to 4.33 eV.[36–39] Corresponding ranges are 4.0 to 4.6 eV for Mo,[36,39,40] 4.52 to 5.10 eV for Ru,[41,42] and 4.15 to 5.11 eV for Rh.[43,44] The present work-function value for ^{99}Tc thus falls within experimental uncertainties in the right range with respect to those of its neighboring $4d$ elements.

B. EELS

Figure 5 displays the $N(E)$ spectrum of ^{99}Tc in a reflection electron energy loss measurement. Its second derivative [marked $N''(E)$] is also presented, for aid in accurately determining the loss peak positions. The energies of the loss peaks for ^{99}Tc are collected in Table I together with those of the other transition elements in period 5. A plot of loss peak energies against the elements is given in Fig. 6 to show the trend among the period-5 transition metals. Technetium has six electrons in its unfilled $4d$ shell and one electron in its $5s$ shell. If one considers these electrons to be free and uses the x-ray data of Marples and Koch,[51] the electronic density N of ^{99}Tc can be calculated. The volume plasmon energy obtained via Eq. (1) is 26.0 eV and the surface plasmon is 18.4 eV in accordance with Eq. (2). The second solid line in Fig. 6 represents the calculated volume plasmons for Y, Zr, Nb, Mo, and Tc and is extended through Ag. The first solid line, on the other hand, represents the corresponding surface plasmon energies obtained from the volume plasmon energies via Eq. (2), while the last two solid lines are drawn through the $N_{II,III}$ and N_I ionization energies for the elements obtained from the x-ray data of Bearden and Burr.[52]

The three-peak structure in the energy range between 20.7 and 25.0 eV in Fig. 5 is believed to be related to the plasmons of ^{99}Tc. These three peaks probably are the result of the overlapping of a surface plasmon peak at $\sim$20.7 eV with a volume plasmon peak at $\sim$25.0 eV, while the middle peak is believed to result from the sum of the overlapped signals. The failure of the measured plasmon peaks to coincide with the calculated ones can be explained in the following ways. First, EELS measures the combination of volume and surface loss signals. If the volume and surface plasmon signals should happen to overlap each other, one may expect a shift of the higher-energy peak (here the volume plasmon peak) to a lower value, and of the lower-energy peak (the surface plasmon peak) to a higher value. This is indeed consistent with what is shown in Fig. 6. Second, ^{99}Tc has atomic number 43 and is located at the center of the group 5 period of transition metals. One expects that the d electrons in this element are not completely free as assumed by the free electron model, and that this will lower the volume plasmon energy from that calculated by the free electron model. Finally, the surface plasmon may be shifted from the value $\hbar\omega_p/\sqrt{2}$ by interband transitions which occur

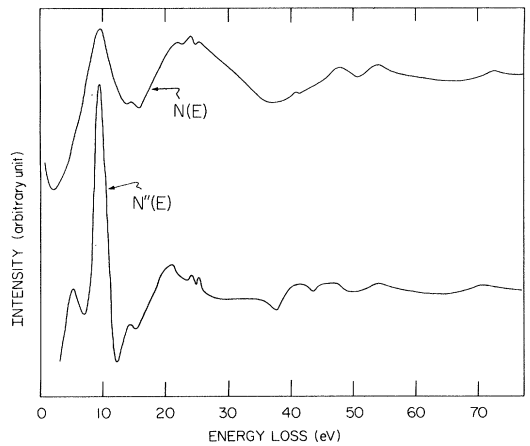

FIG. 5. EDC of electron energy loss of ^{99}Tc (top curve) and its second derivative (bottom curve) from 0 to $\sim$80 eV.

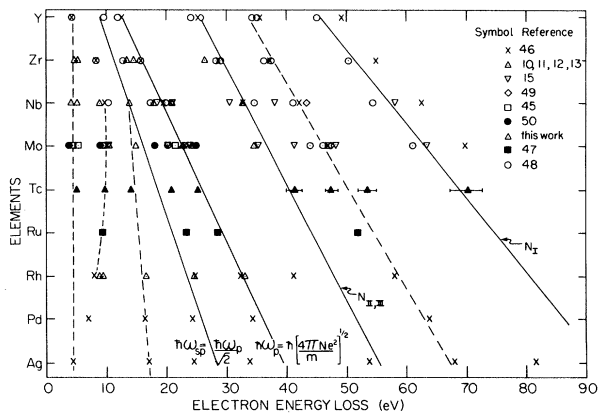

FIG. 6. A plot of loss peak energies against transition-metal element in period 5.

TABLE I. Loss peak energies for transition metals in period 5 are tabulated against the element in order of the periodic table. The sources of data obtained are given in the second column. Volume plasmon energies calculated using the free electron model are given in the last column. In the table columns labeled A, A', and C list interband transition energies; D and E, respectively, are the surface and volume plasmons. B and B', respectively, are the lowered energy surface and volume plasmons; F and F' are $N_{II,III}$ ionization energies; H is an N_I ionization energy; while loss features G and G' lack clear identification as to origin. In the table the superscript r denotes values obtained by analysis of optical reflectivity spectra.

Elements	Ref.	A	A'	B	B'	C	D	E	F	F'	G	G'	H	$\hbar\omega_p$
$_{39}$Y	48	4.1					9.5	11.8	24.0	25.7	34.2	35	45.0	
														12.5
	46	4.0						12.4		25.4		35.6	49.1	
$_{40}$Zr	13			5.2^r	5.7^r		13.4	14.6	26.4					
	48			8.1			12.7	15.7	28.2	29.0	36.2	37.4	50.2	
														15.3
	46			8.0				15.6		28.7		37.2	54.8	
$_{41}$Nb	46				9.5			19.6	32.4			42.0	62.4	
	15				9.6		18.3	20.8	30.3		37.9		57.9	
	48				10.2		17.2	19.8		34.6	41.0		54.3	19.4
	10	4.0	5.1	9.0^r	9.7^r	13.8	17.7	20.8	32.4					
	49				9.9			19.7				43.2		
$_{42}$Mo	46				9.9			22.8				46.8	69.8	
	15				10.2		20.1	23.9	35.2		41.0	48.2	63.4	
	45	4.2	5.1		9.5			21.5				46.8		
	49				10.1			22.4				47.5		23.0
	48				10.3		20.2	23.0			43.8	46.0	61.0	
	50	4.0		9.0			18.0	25.0						
	11			9.5^r	10.4^r	14.8	19.8	24.4	34.6					
$_{43}$Tc	This work		5.0±0.4		9.5±0.5	14.0±0.5	20.7±0.5	25.0±0.5		41.0±1.0	47.5±1.0	53.5±1.5	70.0±2.5	26.0
$_{44}$Ru	47			9.2			23.2	28.5			52.0			
$_{45}$Rh	12			8.8^r	9.0^r	16.5	24.5	33.0						
	46			7.9			24.6	32.2	41.4		57.8			
$_{46}$Pd	46			6.8		16.1	24.2	34.3				63.6		
$_{47}$Ag	46	4.2				17.0	24.4	33.6		53.5		67.7	81.4	

near $\hbar\omega_{sp}$ with considerably more strength than at $\hbar\omega_p$, as was mentioned by Weaver *et al.*[11]

In addition to the volume and surface loss peaks, additional "lowered" volume and surface loss peaks are known for many transition metals,[10–12] as mentioned in Sec. I. For Nb and Mo the lowered plasmon peaks occur near 10 eV. The loss peak at 9.5±0.5 eV in the $N''(E)$ spectrum of Fig. 5 for ^{99}Tc is assigned as the lowered energy plasmon peak. However, the presumably distinct volume and surface components of this lowered plasmon are not resolvable in this experiment as is also the case for Nb and Mo.[10,11,15] The second dashed line in Fig. 6 connects the loss peak energies in all elements from Nb to Rh which correspond to the lowered energy plasmons discussed by Weaver *et al.*[10–13]

The peaks at 5.0 and 14.0 eV are probably due to interband transitions, since similar peaks have been observed for other transition metals in group 5, as are indicated by the first and third dashed lines in Fig. 6. However, Ballu *et al.*[45] found that the intensity of the 4.2- and 5.1-eV loss peaks decreased rapidly when oxygen was adsorbed on a Mo (100) face. They thus suggested that these peaks arise from transitions involving a surface state as initial state. We cannot rule out the possibility that the loss peak at 5.0 eV of our measurement is also surface related. The peaks at 41.0 and 70.0 eV are the $N_{II,III}$ and N_I ionization peaks. The peaks agree well in energy with the x-ray data (the third and fourth solid lines in Fig. 6) of Bearden and Burr.[52] We are not yet clear on the physical origins of the peaks at 47.5 and 53.5 eV. There are lines between the $N_{II,III}$ and N_I ionization lines for other transition elements which seem similar (see the last dashed line in Fig. 6) to these two peaks. One of the possible explanations is that these are multiple loss peaks. For example, a volume plasmon at 25.0±0.5 eV plus a surface plasmon of 20.7±0.5 eV will add up to 45.7±1.0 eV, which may account for the peak at 47.5±1.0 eV. In addition, the $N_{II,III}$ ionization energy 41.0±1.0 eV plus the interband transition at 14.0±0.5 eV will add up to 54.5±1.5 eV, which is the right energy for the peak at 53.5±1.5 eV. It is not always easy to give a physical interpretation for a loss peak. For example, in the paper of Lynch *et al.*[46] the loss peaks at 25.4, 28.7, 32.4, 46.8, 57.8 63.6, and 67.7 eV were assigned to be the $N_{II,III}$ ionizations of Y, Zr, Nb, Mo, Rh, Pd, and Ag. It can easily be seen from Fig. 6 that the first three values lie well with respect to the x-ray data

(the third solid line), while the remaining data are roughly 10 eV higher than the x-ray data, and too far off to be accounted for by experimental uncertainty. These data and the others lie fairly well along the last dashed line whose origin is not yet clear. On the other hand, Zashkvara *et al.*[47] have difficulty interpreting the loss peak at 28.5 eV for Ru. This peak most likely is the volume plasmon as can be seen from Fig. 6, while the peaks at 23.2 and 9.2 eV, which they considered as plasma oscillations, are more likely a surface plasmon peak and the lowered plasmon (including volume and surface modes) discussed by Weaver *et al.* With this reassignment, the volume and surface plasma peaks of Ru are very much like those of ^{99}Tc. In both cases the volume peak is shifted to a lower energy while the surface peak is shifted to a higher energy from the value of the free electron model.

IV. CONCLUSION

Our UPS measurements on ^{99}Tc show that the measured EDC's agree reasonably well with the calculated density of states for technetium. The EELS data of our work on ^{99}Tc and the data on period-5 transition metals from other workers now confirm that a plasma oscillation at a lower energy is a phenomenon common to all elements in transition period 5. Two plasmon modes (one of higher and one of lower energy) are quite common in semiconductors in which two valence bands are available. The plasmon modes obtained by Cazaux[53,54] by using the Lorentz model of the dielectric function agreed quite well with experimental data on $NbSe_2$ and similar compounds. In transition metals, one does not have two valence bands, but, as Weaver *et al.*[10–12] have suggested, one may consider that one group of the electrons is largely *s-p* electrons and the other, the *d* electrons, and plausibly obtain a plasmon from each group as was done by Cazaux. Clearly a more detailed theoretical approach is called for to apply this idea realistically to the transition metals in period 5. Thus, it now appears timely for further theoretical investigations of this general effect. For volume plasmons the free electron model works quite well for this group down to Rh, as is shown in Fig. 6. Larger deviations begin at Pd, in which the $4d$ shell is completely filled. The surface plasmon, on the other hand, deviates generally from that predicted theoretically. The deviation may be explained by the overlap between the volume and surface plasmons which tends to shift their energies closer to each other. Interband transitions may also strongly affect the energy of the surface plasmon.

ACKNOWLEDGMENTS

Ames Laboratory is operated for the U.S. Department of Energy by Iowa State University under Contract No. W-7405-Eng-82. This work was supported by the Director for Energy Research, Office of Basic Energy Sciences, U.S. Department of Energy.

[1]T. P. Chen, E. L. Wolf, and A. L. Giorgi, Surf. Sci. 122, L613 (1982).
[2]S. T. Sekula, R. H. Kernohan, and G. R. Love, Phys. Rev. 155, 364 (1967).
[3]D. Dew-Hughes, Cryogenics 15, 435 (1975).
[4]D. A. Papaconstantopoulos, L. L. Boyer, B. M. Klein, A. R. Williams, V. L. Moruzzi, and J. F. Janak, Phys. Rev. B 15, 4221 (1977).
[5]R. Asokamani, K. Iyakutti, and V. Devanathan, Solid State Commun. 30, 385 (1979).
[6]I. Lindau and W. E. Spicer, J. Appl. Phys. 45, (9), 3720 (1974).
[7]David Bohm and David Pines, Phys. Rev. 82, 625 (1951).
[8]R. H. Ritchie, Phys. Rev. 106, 874 (1957).
[9]For examples, see Refs. 10, 11, and 46.
[10]J. H. Weaver, D. W. Lynch, and C. G. Olson, Phys. Rev. B 7, 4311 (1973).
[11]J. H. Weaver, D. W. Lynch, and C. G. Olson, Phys. Rev. B 10, 501 (1974).
[12]J. H. Weaver, C. G. Olson, and D. W. Lynch, Phys. Rev. B 15, 4115 (1977).
[13]D. W. Lynch, C. G. Olson, and J. H. Weaver, Phys. Rev. B 11, 3617 (1975).
[14]H. Froitzheim in *Electronic Spectroscopy for Surface Analysis,* edited by H. Ibach (Springer, Berlin, 1977), p. 208.
[15]W. K. Schubert and E. L. Wolf, Phys. Rev. B 20, 1885 (1979).
[16]S. K. Sinha and B. N. Harmon, in *Superconductivity in d- and f-band Metals,* edited by D. H. Douglass (Plenum, New York, 1976), p. 269.
[17]J. Ruvalds and L. M. Kahn, Phys. Lett. 70A, 477 (1979).
[18]H. Fröhlich, J. Phys. C 1, 544 (1968).
[19]W. E. Pickett and P. B. Allen, Phys. Lett. 48A, 91 (1974); Phys. Rev. B 13, 1473 (1978).
[20]L. F. Mattheiss, L. R. Testardi, and W. W. Yao, Phys. Rev. B 17, 4640 (1978).
[21]L. Y. L. Shen, Surf. Sci. 66, 239 (1976).
[22]For the description of the discharge lamp, see J. E. Rowe, S. B. Christman, and E. E. Chaban, Rev. Sci. Instrum. 44, 1675 (1973).
[23]Values quoted here are rough measurements obtained from the density-of-states histogram in Ref. 5.
[24]B. J. Waclawski and E. W. Plummer, Phys. Rev. Lett. 29, 783 (1972).
[25]J. E. Demuth, Surf. Sci. 65, 369 (1977).
[26]W. Eberhardt, F. Greuter, and E. W. Plummer, Phys. Rev. Lett. 46, 1085 (1981).
[27]D. E. Eastman and J. K. Cashion, Phys. Rev. Lett. 27, 35 (1971).
[28]R. J. Smith, Phys. Rev. Lett. 45, 1277 (1980).
[29]Shang-Lin Weng, T. Gustafsson, and E. W. Plummer, Phys. Rev. Lett. 44, 344 (1980).
[30]H. Conrad, G. Ertl, J. Kuppers, and E. E. Latta, Surf. Sci. 58, 578 (1978).
[31]Shang-Lin Weng, Phys. Rev. B 25, 6188 (1982).
[32]B. Feuerbacher and B. Fitton, Phys. Rev. Lett. 29, 786 (1972).
[33]F. P. Netzer, Surf. Sci. 102, 75 (1981).
[34]Sergio Trasatti, Surf. Sci. 32, 735 (1972).
[35]H. B. Michaelson, J. Appl. Phys. 21, 536 (1950).
[36]D. E. Eastman, Phys. Rev. B 2, 1 (1970).
[37]Kenneth A. Kress and Gerald J. Lapeyre, in *Electron Density of States,* NBS Special Publication No. 323, edited by L. H. Bennett (U.S. GPO, Washington, D.C., 1971), p. 209.
[38]R. G. Wilson, J. Appl. Phys. 37, 3170 (1966).

[39]O. Milton, Ph.D. thesis, Brown University, 1963.
[40]K. A. Kress and G. J. Lapeyre, Nat. Bur. Stand. (U.S.) Spec. Publ. 3231, 209 (1971).
[41]J. Psarouthakis and R. D. Huntington, Surf. Sci. 7, 279 (1967).
[42]R. Bowman and W. M. H. Sachtler, Surf. Sci. 24, 140 (1971).
[43]M. E. Belyaeva, L. A. Larin, and T. V. Kalish, Elektrokhimiya 12(4), 567 (1976).
[44]B. E. Nieuwenhuys, B. G. Van Aardenne, and W. M. H. Sachtler, Thin Solid Films 17, S7 (1973).
[45]Y. Ballu, J. Lecante, and H. Rousseau, Phys. Rev. B 14, 3201 (1976).
[46]M. J. Lynch and J. B. Swan, Aust. J. Phys. 21, 811 (1968).
[47]V. V. Zashkvara, V. S. Red'kin, and M. I. Korsunskii, Fiz. Tverd. Tela (Leningrad) 11, 2402 (1969) [Sov. Phys.—Solid State 11, 1944 (1970)].
[48]V. V. Zashkvara, M. I. Korsunskii, V. S. Red'kin, and V. E. Masyagin, Fiz. Tverd. Tela (Leningrad) 11, 3667 (1969) [Sov. Phys.—Solid State 11, 3083 (1970)].
[49]R. H. Apholte and K. Ulmer, Phys. Lett. 22, 552 (1966).
[50]M. I. Korunskii, Ya. E. Genkin, S. M. Chanyshev, and E. V. Tsveimah, Fiz. Tverd. Tela (Leningrad) 16, 867 (1974) [Sov. Phys.—Solid State 16, 557 (1974)].
[51]J. A. C. Marples and C. C. Koch, Phys. Lett. 41A, 307 (1972).
[52]J. A. Bearden and A. F. Burr, Rev. Mod. Phys. 39, 125 (1967).
[53]J. Cazaux, Opt. Commun. 3, 221 (1971).
[54]J. Cazaux, Surf. Sci. 29, 114 (1972).